INHIBITION OF CYTOCHROME OXIDASE AND BLUE-LIGHT DAMAGE IN RAT RETINA

Enping Chen

Eye Laboratory,
St. Erik's Eye Hospital
S–112 82 Stockholm* and
Department of Medical Biophysics,
Karolinska Institute
S–104 01 Stockholm, Sweden

* Address for correspondence

** Supported by Karolinska Institute Research Foundation, Edwin Jordans Stiftelse för Oftalmologisk Forskning, the Swedish Society for Medical Research, Birgit Hansson Palmgrens Fond för forskning rörande ögonsjukdomar and Stig och Karin Irvalls Donationsfond för forskning främst rörande allergiska sjukdomar och ögonsjukdomar.

Abstract. The activity of cytochrome oxidase, outer nuclear layer thickness and edema were quantitatively evaluated in the blue–light–exposed rat retina. Dark–adapted or cyclic–light–reared rats were exposed to blue light with a retinal dose of 380 kJ/m^2. Immediately, one, two, and three day(s) after exposure, the retinas of six rats from each adaptation group were examined. There was no difference between the dark–adapted and cyclic–light–reared rats. Immediately after light exposure, cytochrome oxidase activity decreased. The activity in the inner segments remained low at day one, while severe edema was observed in the inner and outer segments. The outer nuclear layer thickness decreased one to three days after exposure. The blue–light exposure inhibited cytochrome oxidase activity and caused retinal injury. Similarity of the injury process in the dark–adapted and cyclic–light–reared retinas suggests that rhodopsin was not involved. The inhibition of cytochrome oxidase could be a cause of retinal damage.

Introduction

The retina can be damaged by chronic optical exposure [14, 15, 21, 22]. The damage mechanism varies depending on the wavelength of applied radiation [10, 16, 21, 24, 25, 27, 32, 34]. Rhodopsin mediates photochemical retinal damage most effectively in the green region [21, 34]. Cytochrome oxidase has been suggested as a target in blue–light [16, 24, 25] and ultraviolet–A radiation retinal damage [27].

Cytochrome oxidase is a key enzyme in the respiratory chain. The retina has high oxygen consumption due to its high metabolic rate and high energy requirement. High cytochrome oxidase activity is observed in the pigment epithelium and the inner segment of the photoreceptors [4].

Blue light exposure with a dose of 240 kJ/m^2 reversibly inhibited oxygen consumption in the isolated bovine pigment epithelium. Judging from the action spectrum, the blue light effect may be mediated by cytochrome oxidase [24, 25]. Blue–light exposure with a retinal dose of 110 kJ/m^2 inhibits cytochrome oxidase activity in rat retina. This inhibition is also reversible [7]. The retina consumes less oxygen in a light environment than in darkness [28]. Considering the reversible inhibition of cytochrome oxidase activity in retina [7] and of the oxygen consumption by retina [24, 25], cytochrome oxidase may be a part of the mechanism for the light–dark regulation of oxygen consumption.

Increased dose causes cellular damage [24, 25]. In vitro blue–light exposure destroys cytochrome oxidase and therefore inhibits cellular respiration [19, 20]. In vivo white–light exposure inhibits the activity of several important enzymes in rat retina including cytochrome oxidase. This inhibition is followed by retinal degeneration [12, 13].

Ultraviolet–A radiation bleaches rhodopsin less efficiently than green light does, and these two spectra produce histologically different damages [27]. This suggests that the mechanism for green–light damage is different from that for shorter wavelengths [27]. The absorption of blue light by rhodopsin is low [33]. However, rhodopsin could still absorb a certain amount of blue–light energy, and may thus trigger a photochemical reaction that finally causes damage. The possible involvement of rhodopsin in blue–light retinal damage was investigated in the present study by comparing the retinal damage in the dark–adapted rats and in the cyclic–light reared rats.

The rats were exposed to blue light (404 $\pm$ 10 nm), as cytochrome oxidase absorbs strongly in the blue light region, with an absorption peak at about 410 nm [1].

The aims of the present study were 1) to evaluate the relation between the inhibition of cytochrome oxidase and blue–light retinal damage and 2) to investigate the significance of rhodopsin in blue–light retinal damage.

Materials and methods

Exposure Device

The light source comprised a 200–W–high–pressure mercury lamp, an interference filter with a maximum transmittance at 404 nm and a half width of 10 nm, and a projection system [29]. In the present study, the projection system was modified by adding a 36–D convex quartz lens in the projection system. The projected radiation had a convergence of 0.7 radians.

EXperimental Procedure

Female Sprague–Dawley rats were obtained from B & K Universal, Sollentuna, Sweden when they were 42–days of age. The rats were randomly divided into a cyclic–light–reared group and a dark–adapted group, each of 24 rats. The cyclic–light–reared group was reared for 7 to 12 days in an animal room where the illumination to the cage was 12 hours' 420 – 580 lux and 12 hours' dark. The rats in both groups were born and raised in the similar light surroundings at B & K Universal. The cyclic–light–reared group stayed in 600 lux illumination at least two hours before exposure to optical radiation. The dark–adapted group was kept for 7 to 12 days in a dark room, with dim red–photographic– safe light only during feeding and anesthesia. Both groups were fed with commercial pellets and had free access to water.

The dark–adapted and the cyclic–light–reared rats were exposed under identical conditions at room temperature, under anesthesia with pentobarbital sodium 40 mg/kg body weight intraperitoneally. The eyelids of the anesthetized rats were opened manually for a while. The palpebral fissure then remained about 4 – 5 mm during exposure without further manipulation. The pupils of both eyes were dilated with tropicamide (5g/l) to about 3 mm in diameter. The

optical radiation was directed to the retinal area just nasal to the optical nerve in the exposed eye, with a cornea–convex–lens distance of 10 mm. The beam position was estimated by observing retina with an ophthalmoscope along the optical axis of the light source for exposure.

The distribution of radiation on the rat retina was observed in an enucleated rat eye. The exposed area was 1.2 mm in diameter.

For each rat, one randomly chosen eye was exposed for about 15 minutes. The other eye was control. The intensity of the optical radiation at the corneal level was measured with a thermopile radiometer whose probe was calibrated to a source traceable to the National Bureau of Standards, USA [29]. The retinal dose was estimated to be 380 kJ/m^2 (380 W/m^2 x 1000 seconds) at a corneal dose of 300 kJ/m^2 (300 W/m^2 x 1000 seconds), a pupil diameter of 3 mm and an exposed retinal area 1.2 mm in diameter. Ocular transmittance at 404 nm was assumed to be 20 % [3]. This dose is too low to cause thermal retinal damage [8].

After the exposure, the rats of both groups were kept in a cyclic–light environment. Six randomly selected rats from each group were sacrificed immediately, one, two and three days after exposure. Both eyes were removed and were serially cryosectioned in the horizontal plane. The section thickness of the retinal section was set at 10 μm on the cryosectioning machine (Leitz–Histo–Kryotom, FRG). The sections from the damaged area of the exposed eye, and from the corresponding area of the control eye, were selected for light–microscopic morphology, morphometry and quantitative histochemistry. Retinal sections about 40 μm thick were used for quantitative microradiography.

The treatment of the rats in the present study was in accordance with the Declaration of Helsinki and the Guiding Principles in the Care and Use of Animals (1989).

Light Microscopic Morphology and Morphometry

The retinal sections were stained with toluidine blue for light–microscopic evaluation and morphometric measurement.

The thickness of the outer nuclear layer of three sections from each eye was measured with a gauge (resolution 0.1 μm) incorporated in a Leitz microscope. The thickness was measured at three randomly chosen locations in the exposed area of the exposed section, and at the corresponding area of the control section.

Quantitative Histochemistry

The retinal sections were stained histochemically for cytochrome oxidase activity [4]. The density of the stain in the pigment epithelium, outer segments and inner segments of the photoreceptors, and in the outer plexiform layer, was measured using a densitometer with a measuring spot of 5 μm in diameter. Three retinal sections from each eye were investigated. Three locations in the exposed area, and at the corresponding area of the control, were measured.

Quantitative Microradiography

Protein and lipid density were determined in the one–day–after–exposure group. Retinal sections from each eye were freeze–dried. Before and after lipid extraction, each section was imaged on a high–resolution photographic emulsion with soft X rays, together with a reference system [5, 17].

The outer and inner segment region in the retinal image was measured with a densitometer. The measuring spot, 19.1 μm in diameter, was centered at the border between the outer segments and inner segments in the control, and was placed at the central part between the pigment epithelium and outer

nuclear layer in the exposed retina. The photometric readings of the retinal section, before and after lipid extraction, were converted to protein, lipid and total dry mass densities [6]. Three locations in the exposed area of the exposed eye, and at the corresponding area of the control, were measured. A mean value was calculated for each section.

Statistical Analysis

The outer nuclear layer thickness, the histochemical staining at the pigment epithelium, outer segments, inner segments and outer plexiform layer, respectively, were analyzed with a mixed effects model (Model 1 in Appendix 1). The model was modified to analyze the variances of the above–mentioned parameters at each post–exposure interval (Model 2 in Appendix 1). The variances of the protein, the lipid, and the total dry mass density at the outer segments and inner segments were also analyzed using a mixed effects model (Model 3 in Appendix 1). The significance level was set at $p = 0.05$.

Results

Morphology

There was no discernible difference in light–microscopic appearance between the dark–adapted and the cyclic–light–reared rats at any post–exposure interval. As observed in light microscopy (Fig. 1), there was no morphologic difference between the exposed retinas and the control retinas immediately after exposure. One day after exposure, the inner segments and outer segments were edematous. Two days after exposure, the inner segments and outer segments were disintegrating. In some regions, the pigment epithelium was invaded by

macrophages. Three days after exposure, the inner segments and outer segments in the exposed area were disintegrated. Macrophages invaded the outer and inner segments region. Some pigment epithelium cells survived to the end of the present observation. No morphologic alteration was found in the control retinas of either group.

Morphometry of ONL Thickness

There was no statistically significant difference in outer nuclear layer thickness between the dark–adapted retinas and the cyclic–light–adapted retinas (Table 1: Adaptations and Int. (α–β)). The exposure decreased the outer nuclear layer thickness in the exposed retinas (Table 1: Exposure) and the decrease differed among post–exposure intervals (Table 1: Intervals and Int. (β–δ)). The adaptations did not affect the outer nuclear layer thickness after exposure (Table 1: Int. (α–δ) and Int. (α–β–δ)).

The decrease in outer nuclear layer thickness after exposure is shown in Figure 2.

Quantitative Histochemistry

There was no statistically significant difference in cytochrome oxidase activity between the dark–adapted and the cyclic–light–adapted retinas in the pigment epithelium, outer segments, inner segments and outer plexiform layer (Table 2: Adaptations and Int. (α–β)). The exposure caused a significant change in cytochrome oxidase activity in the four layers (Table 2: Exposure), and the changes differed at various post–exposure intervals (Table 2: Intervals and Int. (β–δ)). The adaptations did not affect the cytochrome oxidase activity after the exposure (Table 2: Int. (α–δ) and Int. (α–β–δ)).

The alteration of cytochrome oxidase activity after exposure in the

pigment epithelium, the outer segments, the inner segments and the outer plexiform layer is shown in Figure 3.

Quantitative Microradiography

There was no significant difference between the dark–adapted group and the cyclic–light–reared group in the protein, the lipid or the total dry mass densities (Table 3: Adaptations). Significant decreases in the protein and the total dry mass density were found in the outer segments and inner segments of the exposed retinas one day after the exposure (Table 3: Exposure). However, there was no significant change in the lipid density after the exposure (Table 3: Exposure). The adaptation did not affect the dry mass density after the exposure (Table 3: Int. (α–γ)).

The mean densities of the protein, the lipid and the total dry mass in inner and outer segments one day post–exposure are shown in Figure 4.

Discussion

The present study related cytochrome oxidase inhibition and rhodopsin level to the retinal damage caused by 404–nm–blue–light exposure. Dark–adapted rat retinas have a higher rhodopsin concentration than the retina of rats reared in cyclic light of 12 hours' 40 – 60 lux [23], or 12 hours' 400 lux [26] and 12 hours' dark. In the present study, the cyclic–light–reared group was reared in 12 hours' 420 – 580 lux and 12 hours' dark environment. Therefore, a difference in rhodopsin level between the two groups could be expected. The blue–light injury was quantitatively monitored with regard to cytochrome oxidase activity, outer nuclear layer thickness, protein and lipid density. No difference was found between the dark–adapted and the cyclic–light–reared groups. This suggests that rhodopsin may not be involved in blue–light–retinal damage.

Other damage mechanisms, e.g., the inhibition of enzymes in the retina, may be involved.

In the present study, the assumed transmittance of rat ocular media, 0.2, was derived from human specimens [3]. Rat eyeballs are smaller than human eyeballs. Hence the rat eye has a shorter optical path, and might have a higher transmittance to optical radiation. The rat lens has a transmittance of 0.8 at 400 nm [9], whereas the human lens has a transmittance of about 0.5. Further, the sclear, choroid and retina of the albino rats contain little pigments. The optical radiation may pass through these layers and scatter in the ocular media, and thus increase the retinal irradiance. Therefore, the retinal dose may be underestimated in the present study.

cytochrome oxidase was observed as an indicator of cellular metabolism. In a previous study, cytochrome oxidase activity in the pigment epithelium, outer segments, inner segments and outer plexiform layer recovered after an immediate inhibition by blue–light exposure with a dose of 110 kJ/m^2. No other discernible morphologic alteration followed this recovery [7].

In the present study, the retinal dose was increased to 380 kJ/m^2. Immediately, and one day, after exposure, the cytochrome oxidase activity in the inner segments was inhibited and hence the oxidative respiration and cellular metabolism in the layer were also suppressed. This prolonged suppression of respiration may cause a decrease in the energy supply to the Na^+,K^+–ATPase, and may thereby result in an accumulation of intracellular fluid [18]. Expansion of the cellular membrane during the formation of edema separates the reaction sites of enzyme systems on the cellular membrane, and further disturbs the enzymatic activities [18]. It has been estimated that a 25 % increase in cellular volume causes irreversible damage [18].

In the present study, the inhibition of cytochrome oxidase was accompanied by a half decrease in the total dry mass density in the inner and outer segments region (Fig. 4, Table 3). This suggests a one–to–one dilution of

cellular content, therefore a 100 % increase in volume. The severe edema was followed by a disintegration of the photoreceptor cells, manifested by a gradual decrease in the outer nuclear layer thickness (Fig. 2, Table 1).

It was expected that the cytochrome oxidase in the edematous region would also be diluted. This was shown in the further reduction of cytochrome oxidase activity in inner segments one day after exposure (Fig. 3IS). A significant decrease in protein density was found after exposure. However, there was no significant reduction in lipid density after exposure. The accumulation of lipids in the outer segments and inner segments may come possibly from the disintegrating outer plexiform layer.

The cytochrome oxidase activity in the outer plexiform layer increased over previous level one day after exposure (Fig. 3OP) and the surviving pigment epithelial cells (Fig. 3PE). These retinal elements were not destroyed during the present three–day observation. Increase in cytochrome oxidase activity in these elements may indicate a metabolic compensation for repair of the injury. This repair mechanism could be one of the reasons that the outer plexiform layer and some pigment epithelial cells outlived the photoreceptor cells after the exposure.

The inner and outer segments were destroyed by the exposure. The destroyed mitochondria in inner segments and disintegrated outer segments membrane could have released the membrane–bound cytochrome oxidase. High activity of the solubilized cytochrome oxidase [31] may explain the increased cytochrome oxidase activity in the region of the disintegrated inner and outer segments (Fig. 3OS and IS). Futher, cytochrome oxidase activity of the macrophages [12], which invaded in the disintegrating inner and outer segments, may contribute to the increased cytochrome oxidase activity in this region.

In the present study, blue–light exposure inhibited the cytochrome oxidase activity in the rat retina. The prolonged inhibition of the cytochrome oxidase in the inner segments was followed by destruction of photoreceptor

cells. Rhodopsin may be insignificant in blue–light–retinal injury. Hence, inhibition of cytochrome oxidase by blue–light exposure and the consequent suppression of the cellular metabolism is a potential cause of retinal degeneration. This assumption would be further tested by correlating the action spectrum for cytochrome oxidase activity with the absorption spectrum for cytochrome oxidase.

Acknowledgements

The author would like to thank Dr Per Söderberg, Professor Bo Lindström and Professor Myron L. Wolbarsht for comments on the manuscript, Mr Lennart Wallerman and Mr Ove Kristenson for help with experimental devices, Mrs Wen Qian for computer programming, and Mr Tim Crosfield for correcting linguistic errors.

References

1. Bell JE and Hall C (1981) Hemoproteins. In: Bell JE (Ed) Spectroscopy in biochemistry. CRC Press Inc, Boca Raton, Florida, pp 42–46
2. Bennett CA and Franklin NL (1963) Analysis involving both types of classifications. In: Statostical analysis in chemistry and the chemical industry. John Wiley & Sons Inc, New York, pp 410–417
3. Boettner EA and Wolter JR (1962) Transmission of the ocular media. Invest. Ophthalmol. 1:776–783.
4. Chen E, Söderberg PG and Lindström B (1989) Activity distribution of cytochrome oxidase in the rat retina – A quantitative histochemical study. Acta Ophthalmol (Copenhagen) 67:645–651
5. Chen E, Chung JH, Söderberg PG and Lindström B (1991) Microradiographical determination of the dry mass density in the rat retina. Ophthalmic Res 23:33–39

6. Chen E, Söderberg PG and Lindström B (1991) Lipid and protein density in the rat retina – A microradiographical study. Ophthalmic Res 23:220–224

7. Chen E, Söderberg PG and Lindström B (1992) Cytochrome oxidase activity in rat retina after exposure to 404 nm blue light. Curr Eye Res 11:825–831

8. Clarke AM, Geeraets WJ and Ham WT (1969) An equilibrium thermal model for retinal injury from optical sources. Appl Opt 8:1051–1054

9. Gorgels TGM and Van Norren D (1992) Spectral transmittance of the rat lens. Vision Res 32:1509–1512

10. Ham WTJr, Mueller HA, Sliney DH (1976) Retinal sensitivity to damage from short wavelength light. Nature 260:153–155

11. Ham WTJr, Mueller HA, Ruffolo JJJr and Clarke AM (1979) Sensitivity of the retina to radiation damage as a function of wavelength. Photochem Photobiol 29:735–743

12. Hansson HA (1970) A histochemical study of oxidative enzymes in rat retina damaged by visible light. Exp Eye Res 9:285–296

13. Hansson HA (1971) A histochemical study of cellular reactions in rat retina transiently damaged by visible light. Exp Eye Res 12:270–274

14. Friedman E and Kuwabara T (1968) The retinal pigment epithelium – IV. The damaging effects of radiant energy. Arch Ophthal 80:265–279

15. Gorn RA and Kuwabara T (1967) Retinal damage by visible light – A physiologic study. Arch Ophthal 77:115–118

16. Lawwill T (1982) Three major pathologic processes caused by light in the primate retina: a search for mechanisms. Tr Am Ophth Soc 80:517–579

17. Lindström B (1955) Roentgen absorption spectrophotometry in quantitative cytochemistry. Acta Radiologica Suppl 125

18. Macknight ADC (1984) Cellular response to injury. In: Staub NC and Taylor AE (Eds) Edema. Raven Press, New York, pp 489–520

19. Ninnemann H, Butler WL and Epel BL (1970) Inhibition of respiration in yeast by light. Biochim Biophys Acta 205:499–506

20. Ninnemann H, Butler WL and Epel BL (1970) Inhibition of respiration and destruction of cytochrome a_3 by light in mitochondria and cytochrome oxidase from beef heart. Biochim Biophys Acta 205:507–512

21. Noell WK, Walker VS, Kang BS and Berman S (1966) Retinal damage by light in rats. Invest Ophthalmol 5:450–473

22. Noell WK (1979) Effects of environmental lighting and dietary vitamin A on the vulnerability of the retina to light damage. Photochem Photobiol 29:717–723

23. Organisciak DT, Jiang YL, Wang HM, Pickford M and Blanks JC (1989) Retinal light damage in rats exposed to intermittent light – Comparison with continuous light exposure. Invest Ophthalmol Vis Sci 30:795–805

24. Pautler EL Morita M and Beezley D (1989) Reversible and irreversible blue light damage to the isolated, mammalian pigment epithelium. In: LaVail MM, Hollyfield JG and Anderson RE (Eds) Inherited and environmentally induced retinal degenerations. Alan R Liss Inc, New York, pp 555–567

25. Pautler EL, Morita M and Beezley D (1990) Hemoprotein(s) mediate blue light damage in the retinal pigment epithelium. Photochem Photobiol 51:599–605

26. Penn JS and Anderson RE (1991) Effects of light history on the rat retina. In: Osborne NN and Chader GJ (Eds) Progress in retinal research. Pergamon Press, Oxford, pp 75–98

27. Rapp LM, Tolman BL and Dhindsa HS (1990) Separate mechanisms for retinal damage by ultraviolet–A and mid–visible light. Invest Ophthalmol Vis Sci 31:1186–1190

28. Stefansson E, Wolbarsht ML and Landers MBIII (1983) In vivo O_2

consumption in rhesus monkeys in light and dark. Exp Eye Res 37: 251–256

29. Söderberg PG (1990) Experimental cataract induced by ultraviolet radiation. Acta Ophthalmol (Copenhagen) Suppl 196

30. Tso MOM (1973) Photic maculopathy in rhesus monkey: A light and electron microscopic study. Invest Ophthalmol 12:17–34

31. Thompson DA, Suarez–Villafane M and Ferguson–Miller S (1982) The active form of cytochrome c oxidase – effects of detergent, the intact membrane, and radiation inactivation. Biophys J 37:285–292

32. Van Norren D and Schellekens P (1990) Blue light hazard in rat. Vision Res 30:1517–1520

33. Wald G and Brown PK (1958) Human rhodopsin. Science 127:222–226

34. Williams TP and Howell WL (1983) Action spectrum of retinal light–damage in albino rats. Invest Ophthalmol Vis Sci 24:285–287

Appendix

The outer nuclear layer thickness, and the optical density of the histochemical staining in each retinal layer were analyzed with a mixed effects model [2]:

$$x_{ijklmn} = \mu + \alpha_i + \beta_j + C_{k(ij)} + \delta_l + (\alpha\beta)_{ij} + (\beta\delta)_{jl} + (\alpha\delta)_{il}$$

$$+ (\alpha\beta\delta)_{ijl} + (C\delta)_{kl(ij)} + E_{m(ijkl)} + \epsilon_{n(ijklm)} \qquad \text{(Model 1)}$$

Here, each reading, x_{ijklmn}, equals the sum of the expected mean, μ, a term for the adaptations, α_i ($i = 1 .. 2$), a term for post–exposure intervals, β_j ($j = 1 ... 4$) , a term for rats within adaptations and intervals, $C_{k(ij)}$ ($k = 1 ... 6$), a term for exposure, δ_l ($l = 1 ... 2$), a term for interaction between adaptations and intervals, $(\alpha\beta)_{ij}$, a term for interaction between intervals and exposures $(\beta\delta)_{jl}$, an term for interaction between adaptations and exposures, $(\alpha\delta)_{il}$, a term for

interaction among adaptations, intervals and exposures, $(\alpha\beta\delta)_{ijl}$, a term for interaction between rats and exposures within adaptation and interval, $(C\delta)_{kl(ij)}$, a term for sections within eye, $E_{m(ijkl)}$ (m = 1 ... 3), and a term for locations within, $\epsilon_{n(ijklm)}$ (n = 1 ... 3).

For analysis of variance at each interval, the terms of the variation related to post–exposure intervals were removed, and the modified model became:

$$x_{ijklmn} = \mu + \alpha_i + C_{k(i)} + \delta_l + (\alpha\delta)_{il} + (C\delta)_{kl(i)} + E_{m(ikl)} + \epsilon_{n(iklm)} \qquad \text{(Model 2)}$$

The protein, lipid, and total dry mass density one day post–exposure was analyzed with a mixed effects model [2]:

$$x_{ijk} = \mu + \alpha_i + B_{j(i)} + \gamma_k + (\alpha\gamma)_{ik} + (B\gamma)_{jk(i)} + \epsilon_{(ijk)} \qquad \text{(Model 3)}$$

Each reading, x_{ijk}, equals the sum of the expected mean, μ, a term for adaptations, α_i (i = 1 ... 2), a term for rats within each adaptation, $B_{j(i)}$ (j = 1 ... 6), a term for exposures, γ_k (k = 1 ... 2), a term for interaction between adaptations and exposures, $(\alpha\gamma)_{ik}$, a term for interaction between rats and exposures within adaptation, $(B\gamma)_{jk(i)}$, and a term for random error of measurements, $\epsilon_{(ijk)}$.

Table 1
Analysis of variance for outer nuclear layer thickness after blue–light exposure

Source of variance	DF	Sum of squares (μm^2)	Mean square (μm^2)	Expected mean square	$F_{f_1;f_2}(0.95)$
Adaptations (α)	1	8.8	8.8	$\sigma^2_\epsilon + n\sigma^2_E + den\sigma^2_C + bcden\kappa^2_\alpha$	
			<u>0.11</u>		5.42
Intervals (β)	3	24636.7	8212.2	$\sigma^2_\epsilon + n\sigma^2_E + den\sigma^2_C + acden\kappa^2_\beta$	
			<u>98.5</u>		3.46
Rats (C)	40	3334.2	83.4	$\sigma^2_\epsilon + n\sigma^2_E + den\sigma^2_C$	
Exposure (δ)	1	77721.6	77721.6	$\sigma^2_\epsilon + n\sigma^2_E + en\sigma^2_{C\delta} + abcen\kappa^2_\delta$	
			<u>1295.4</u>		5.42
Int. (α–β)	3	49.5	16.5	$\sigma^2_\epsilon + n\sigma^2_E + den\sigma^2_C + cden\kappa^2_{\alpha\beta}$	
			<u>0.20</u>		3.46
Int. (β–δ)	3	29049.7	9683.2	$\sigma^2_\epsilon + n\sigma^2_E + en\sigma^2_{C\delta} + acen\kappa^2_{\beta\delta}$	
			<u>161.4</u>		3.46
Int. (α–δ)	1	0.2	0.2	$\sigma^2_\epsilon + n\sigma^2_E + en\sigma^2_{C\delta} + bcen\kappa^2_{\alpha\delta}$	
			<u>0.003</u>		5.42
Int. (α–β–δ)	3	276.2	92.0	$\sigma^2_\epsilon + n\sigma^2_E + en\sigma^2_{C\delta} + cen\kappa^2_{\alpha\beta\delta}$	
			<u>1.53</u>		3.46
Int. (C–δ)	40	2401.7	60.0	$\sigma^2_\epsilon + n\sigma^2_E + en\sigma^2_{C\delta}$	
			<u>1.68</u>		1.53
Sections (E)	192	6854.6	35.7	$\sigma^2_\epsilon + n\sigma^2_E$	
Locations (ϵ)	576	8917.5	15.5	σ^2_ϵ	

DF: Degrees of freedom. $F_{f_1;f_2}(0.95)$: The significance limit according to the F distribution (significance level = 0.05). α: Adaptations; β: Post–exposure intervals; C: Rats; δ: Exposures; Int.: Interaction; E: Sections; ϵ: Locations. a = 2 = The adaptations; b = 4 = The post–exposure intervals; c = 6 = The number of rats in each interval within each adaptation group; d = 2 = The exposure and control; e = 3 = The number of sections within each eye; n = 3 = The number of locations. Underlined numeric values: the test statistics. σ^2 = The expected variance of the indexed–random source. κ^2 = A factor corresponding to the variance of the indexed–fixed sources.

Table 2

Analysis of variance for cytochrome oxidase activity in pigment epithelium, outer segments, inner segments and outer plexiform layer after blue–light exposure

Source of variance	DF	Mean square (AU^2)				Expected mean square	$F_{f_1;f_2}(0.95)$
		PE	OS	IS	OP		
Adaptations (α)	1	0.04	0.01	0.33	0.04	$\sigma^2_\epsilon + n\sigma^2_E + den\sigma^2_C + bcden\kappa^2_\alpha$	
		0.13	0.03	1.50	0.44		5.42
Intervals (β)	3	8.46	10.33	13.96	0.81	$\sigma^2_\epsilon + n\sigma^2_E + den\sigma^2_C + acden\kappa^2_\beta$	
		26.44	31.30	63.46	9.00		3.46
Rats (C)	40	0.32	0.33	0.22	0.09	$\sigma^2_\epsilon + n\sigma^2_E + den\sigma^2_C$	
Exposure (δ)	1	3.15	7.98	2.30	0.87	$\sigma^2_\epsilon + n\sigma^2_E + en\sigma^2_{C\delta} + abcen\kappa^2_\delta$	
		7.00	22.17	10.00	10.88		5.42
Int. (α–β)	3	0.27	0.38	0.06	0.16	$\sigma^2_\epsilon + n\sigma^2_E + den\sigma^2_C + cden\kappa^2_{\alpha\beta}$	
		0.84	1.15	0.27	1.78		3.46
Int. (β–δ)	3	7.77	8.99	12.13	0.92	$\sigma^2_\epsilon + n\sigma^2_E + en\sigma^2_{C\delta} + acen\kappa^2_{\beta\delta}$	
		17.27	24.97	52.74	11.50		3.46
Int. (α–δ)	1	0.03	0.25	0.04	0.13	$\sigma^2_\epsilon + n\sigma^2_E + en\sigma^2_{C\delta} + bcen\kappa^2_{\alpha\delta}$	
		0.07	0.69	0.17	1.63		5.42
Int. (α–β–δ)	3	0.03	0.15	0.02	0.04	$\sigma^2_\epsilon + n\sigma^2_E + en\sigma^2_{C\delta} + cen\kappa^2_{\alpha\beta\delta}$	
		0.07	0.42	0.09	0.50		3.46
Int. (C–δ)	40	0.45	0.36	0.23	0.08	$\sigma^2_\epsilon + n\sigma^2_E + en\sigma^2_{C\delta}$	
		3.00	2.12	1.64	1.14		1.53
Sections (E)	192	0.15	0.17	0.14	0.07	$\sigma^2_\epsilon + n\sigma^2_E$	
Locations (ϵ)	576	0.05	0.04	0.04	0.02	σ^2_ϵ	

DF: Degrees of freedom. AU: Absorption unit. PE: Pigment epithelium. OS: Outer segment of photoreceptors. IS: Inner segment of photoreceptors. OP: Outer plexiform layer. $F_{f_1;f_2}(0.95)$: The significance limit according to the F distribution (significance level = 0.05). α: Adaptations; β: Post–exposure intervals; C: Rats; δ: The exposures; Int. = Interaction; E: Sections; ϵ: Locations. a = 2 = The adaptations; b = 4 = The post–exposure intervals; c = 6 = The number of rats in each interval within each adaptation group; d = 2 = The exposure and control; e = 3 = The number of sections within each eye; n = 3 = The number of locations within each section. Underlined numeric values: the test statistics. σ^2 = The expected variance of the indexed–random term. κ^2 = A factor corresponding to the variance of the indexed–fixed source.

Table 3
Analysis of variance for protein, lipid and
total dry mass densities in the outer and inner segments
one day after blue–light exposure

Source of variance	DF	Mean square $(Kg/m^3)^2$ Protein	Lipid	TDM	Expected mean square	$F_{f_1;f_2}(0.95)$
Adaptations (α)	1	0.0016	0.0003	0.0005	$\sigma^2_\epsilon+\sigma^2_{B\gamma}+n\sigma^2_B+bn\kappa^2_\alpha$	
		2.00	0.60	1.25		6.94
Rats (B)	10	0.0008	0.0005	0.0012	$\sigma^2_\epsilon+\sigma^2_{B\gamma}+n\sigma^2_B$	
Exposures (γ)	1	0.0779	0.0002	0.0864	$\sigma^2_\epsilon+\sigma^2_{B\gamma}+ab\kappa^2_\gamma$	
		779.00	0.67	216.00		6.94
Int. (α–γ)	1	0.0001	0.0007	0.0003	$\sigma^2_\epsilon+\sigma^2_{B\gamma}+b\kappa^2_{\alpha\gamma}$	
		1.00	2.33	0.75		6.94
Int. (B–γ) and error (ϵ)	10	0.0001	0.0003	0.0004	$\sigma^2_\epsilon+\sigma^2_{B\gamma}$	

DF: Degrees of freedom. TDM: Total dry mass. $F_{f_1;f_2}(0.95)$: The significance limit according to F distribution (significance level = 0.05). α: Adaptations; B: Rats; γ: Exposure; ϵ: Random error of measurements. Int. = Interaction. a = 2 = Adaptations; b = 6 = Number of rats within each adaptation; n = 2 = exposure; Underlined numeric value: the test statistics. σ^2 = The expected variance of the indexed–random term. κ^2 = A factor corresponding to the variance of the indexed–fixed source.

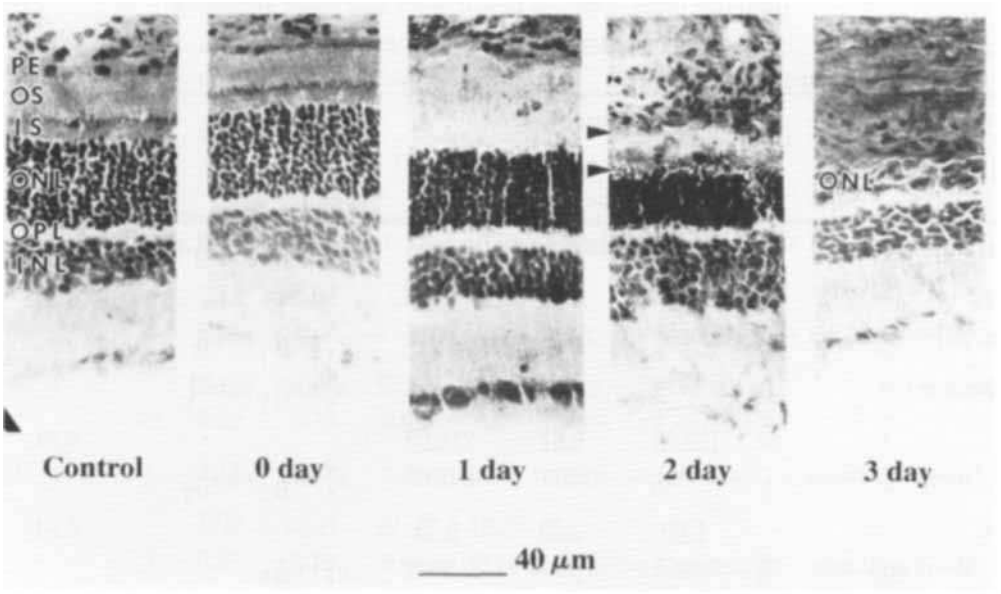

Fig. 1. Toluidine–blue–stained cryosection of rat retina after blue–light exposure. PE: pigment epithelium; OS: outer segments; IS: inner segments; ONL: outer nuclear layer; OPL: outer plexiform layer; INL: inner nuclear layer; Arrow heads: borders of the region of the disintegrating outer and inner segments. Immediately after exposure, there was no observable morphologic alteration. One day after exposure, the inner segments and outer segments were edematous, while there was no observable change in the pigment epithelium. Two days after exposure, the inner and outer segments were disintegrating, and the thickness the outer nuclear layer was decreasing. Macrophages invaded in pigment epithelium. Three days after exposure, the inner and outer segments were disintegrated, and the outer nuclear layer was reduced to two to three nuclei.

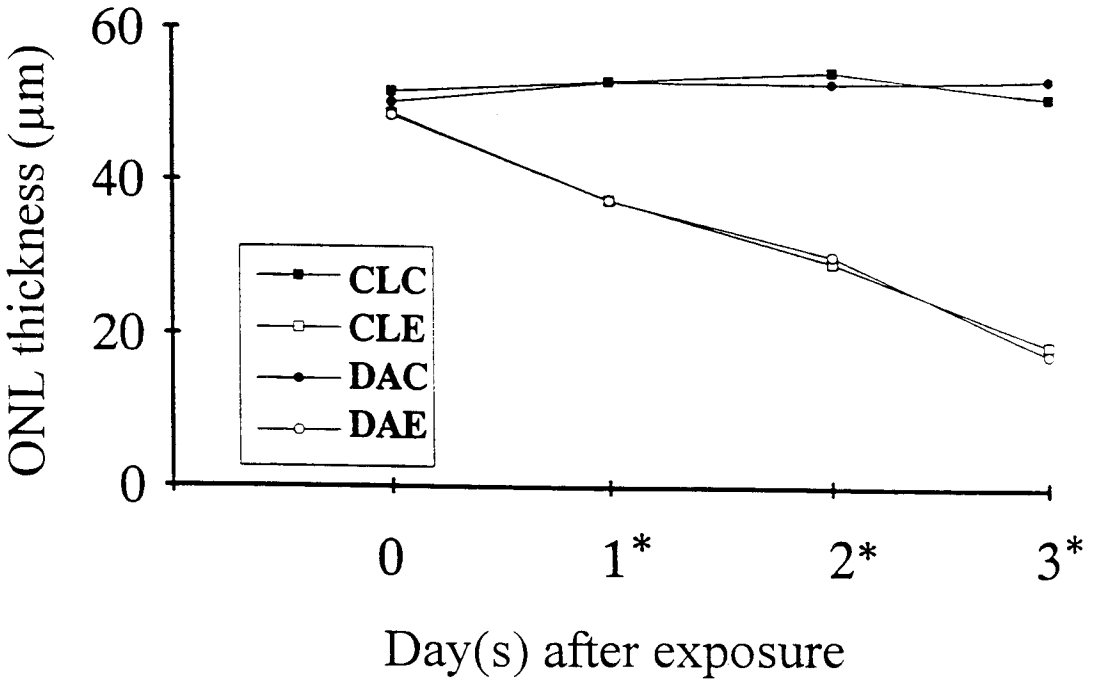

Fig. 2. The thickness of the outer nuclear layer (ONL) after blue–light (404 nm) exposure. 0 day: immediately after exposure. CLC: cyclic–light–reared control; CLE: cyclic–light–reared exposed; DAC: dark–adapted control; DAE: dark–adapted exposed. Each data point is the mean of six eyes. *: statistically significant difference between the exposed and control ($p < 0.05$).

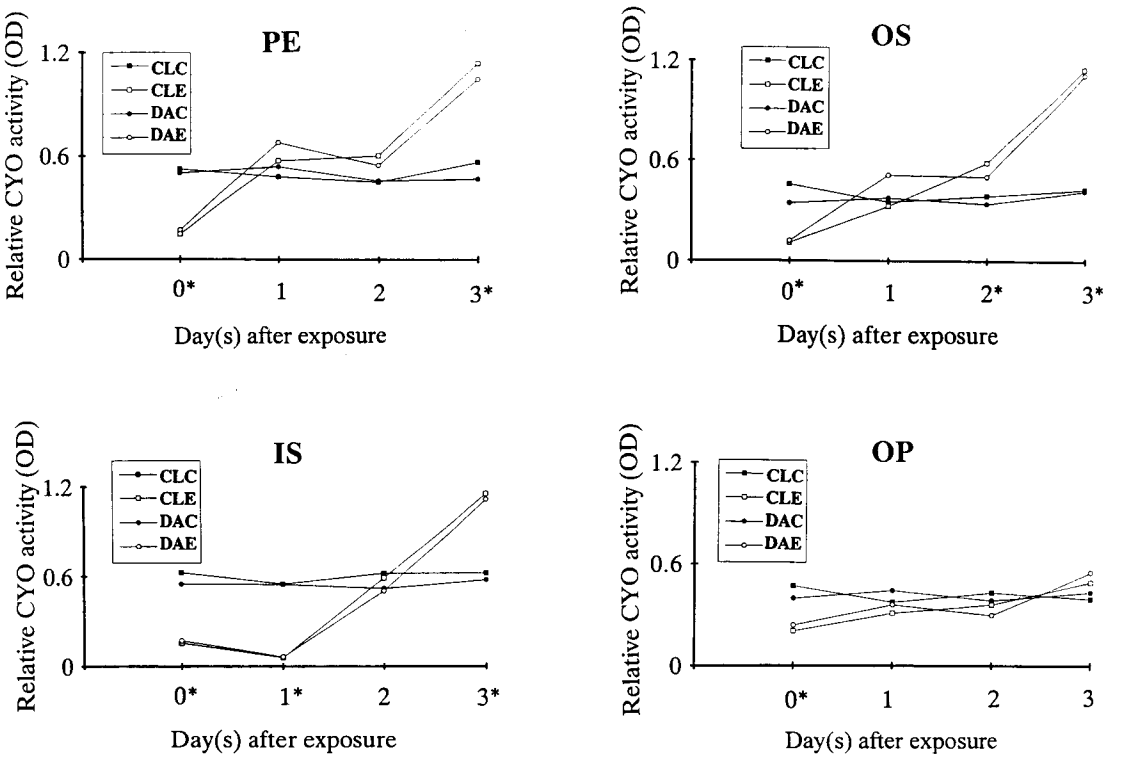

Fig. 3. The activity of cytochrome oxidase in pigment epithelium (PE), outer segments (OS), inner segments (IS) and outer plexiform layer (OP) after exposure to blue light (404 nm). OD: optical density. 0 day: immediately after exposure. CLC: cyclic–light–reared control; CLE: cyclic–light–reared exposed; DAC: dark–adapted control; DAE: dark–adapted exposed. Each data point is the mean of six eyes. *: Statistically significant difference between the exposed and control ($p < 0.05$).

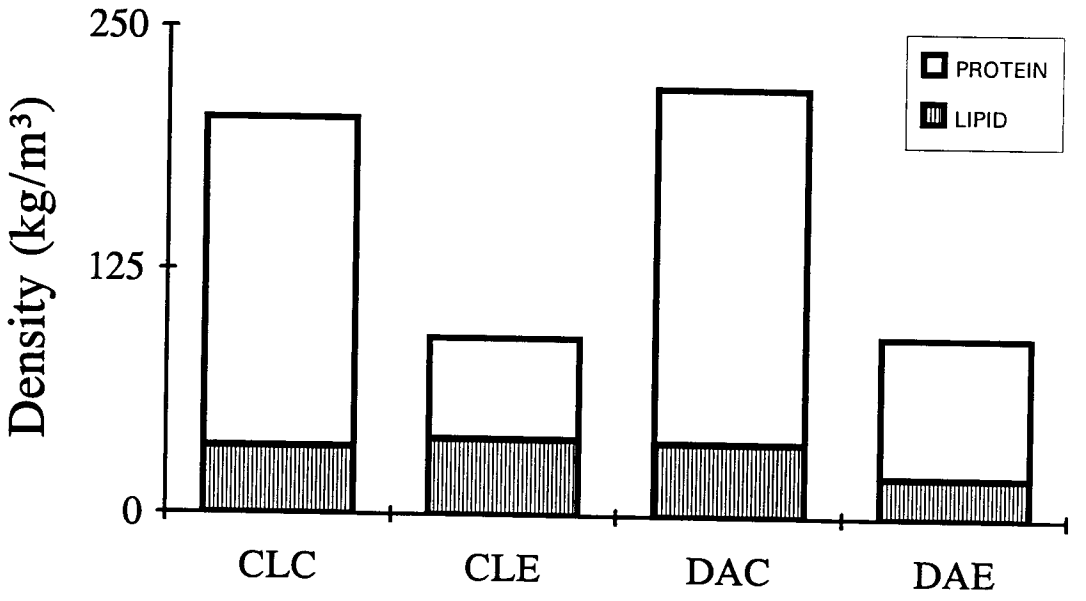

Fig. 4. Lipid and protein density in the region of the inner and outer segment of photoreceptors one day after exposure. Lipid + protein = total dry mass. CLC: cyclic–light–reared control; CLE: cyclic–light–reared exposed; DAC: dark–adapted control; DAE: dark–adapted exposed. Each value is the mean of six eyes.